Zero : Jurnal Sains, Matematika, dan Terapan
E-ISSN : 2580-5754; P-ISSN : 2580-569X
Volume 10, Number 1, 2026
DOI: 10.30829/zero.v10i1.28376
Page: 114 - 123

Local Stability Analysis of Leptospirosis SEITR - SI Model with the Influence of Hydroclimatic Rate and Treatment

[1] **Ega Ananta Erlangga**
Department of Mathematics, Universitas Negeri Surabaya, Surabaya, 60231, Indonesia

[2] **Budi Priyo Prawoto**
Department of Mathematics, Universitas Negeri Surabaya, Surabaya, 60231, Indonesia

Article Info

Article history:

Accepted 25 January 2026

Keywords:

Leptospirosis;
Model SEITR – SI;
Routh – Hurwitz.

ABSTRACT

Leptospirosis is a zoonotic disease whose transmission is influenced by interactions between humans, vectors, and environmental conditions. This study proposes a novel SEITR–SI model that simultaneously integrates treatment dynamics and hydroclimate-dependent transmission within a single analytically tractable framework. Unlike previous SEIR–SI and SIR–SI formulations that either exclude treatment or incorporate hydroclimatic effects through explicit environmental compartments, the proposed model represents hydroclimatic influence implicitly through transmission intensity while preserving mathematical simplicity. The local stability of the disease-free and endemic equilibria is analyzed using the basic reproduction number R_0 and the Routh–Hurwitz criterion. The analysis confirms classical threshold behavior governed by R_0, while numerical simulations reveal that increased hydroclimatic transmission intensity elevates endemic infection levels even under higher treatment rates. These findings highlight that treatment alone may be insufficient in hydroclimate-sensitive environments and underscore the importance of integrated control strategies combining medical intervention with environmental and vector management.

Corresponding Author:

Budi Priyo Prawoto,
Department of Mathematics,
Universitas Negeri Surabaya, Surabaya, Indonesia
budiprawoto@unesa.ac.id

1. INTRODUCTION

Leptospirosis is a zoonotic disease caused by the pathogenic bacterium Leptospira interrogans, which is transmitted to humans through direct or indirect contact with water or soil contaminated by the urine of infected animals, particularly rodents [1], [2], [3], [4], [5], [6]. This disease is commonly reported in tropical and subtropical regions with high rainfall, including Indonesia, where frequent flooding and poor sanitation increase human exposure to contaminated environments [7], [8], [9], [10]. Rodents such as rats play a central role as reservoir hosts, especially in densely populated urban areas, where environmental conditions support high rodent population density and sustained transmission [11], [12].

Leptospirosis presents a diagnostic challenge due to its nonspecific clinical symptoms, which often resemble other infectious diseases such as dengue, malaria, or influenza [13], [14], [15], [16], [17]. Data from the Ministry of Health of the Republic of Indonesia shows that in 2024 there were 1,506 cases of leptospirosis reported by sixteen provinces. Of the reported cases, there were 121 deaths with a case fatality rate (CFR) of 8.03% [18]. These conditions highlight the importance of understanding the mechanisms driving leptospirosis spread, particularly the role of environmental and hydroclimatic factors.

The main factor in the spread of leptospirosis is contaminated stagnant water [19], [20]. Mathematical modeling has therefore become an essential framework for analyzing disease dynamics and evaluating intervention strategies [21], [22], [23]. Previous compartmental models such as the SEIR–SI model in [24] incorporate exposed human classes, while the SIR–SI model in [25] introduces hydroclimatic effects through explicit rate modifications in infected rodents. However, these approaches either neglect treatment dynamics or incorporate hydroclimatic influences through additional environmental compartments or explicit time-dependent climate data, which increases model complexity and may limit analytical tractability.

To address these limitations, this study proposes a SEITR–SI model that integrates treatment dynamics while incorporating hydroclimatic influences implicitly through a hydroclimate-dependent transmission rate, without introducing additional environmental compartments. Unlike [24], which focuses on exposed human compartments without incorporating treatment effects into the stability framework, and [25], which models hydroclimatic effects explicitly through modified rodent infection rates, the proposed formulation integrates treatment dynamics within the same analytical structure while preserving tractability. In contrast to [25], where hydroclimatic variability directly alters transmission structure, the present model maintains a constant threshold formulation for R_0 while allowing hydroclimatic transmission intensity to influence endemic persistence levels.

Despite these developments, limited attention has been given to simultaneously integrating treatment dynamics and hydroclimate-dependent transmission within a unified and analytically tractable SEITR–SI framework. Understanding this interaction is important in hydroclimate-sensitive regions, where environmentally driven transmission may counteract medical interventions.

The primary objective of this study is to analyze the local stability of equilibrium points and to investigate how variations in treatment rate and hydroclimatic transmission intensity affect disease persistence. Numerical simulations are conducted to validate analytical results and to explore parameter sensitivity. The findings suggest that although treatment reduces infection prevalence, strong hydroclimatic transmission intensity can sustain endemic conditions, highlighting the necessity of integrated strategies combining medical treatment with environmental and vector control in hydroclimate-sensitive regions.

2. RESEARCH METHOD

2.1 Model Structure

The SEITR–SI model consists of two populations, namely humans and rat vectors. The model is first formulated with a general hydroclimate-dependent transmission rate to capture hydroclimatic influences. In the human population there are susceptible (S_h), exposed (E_h), infected (I_h), treated (T_h), and recovered (R_h) compartments. The vector population consists of susceptible (S_v) and infected (I_v) rats.

Hydroclimatic influence is incorporated through a hydroclimate-dependent transmission parameter β_h, representing environmental transmission intensity from infected vectors to susceptible humans. In this study, β_h is treated as a constant parameter reflecting average hydroclimatic conditions rather than an explicit time-dependent function of rainfall or flooding data. This assumption preserves analytical tractability while allowing qualitative assessment of hydroclimatic effects through variations in transmission intensity.

The model is constructed under the following assumptions: 1) all populations are closed, 2) the total human and vector populations are constant, 3) There is no population migration, 4) Transmission only occurs from vectors to humans, 5) Infected humans can undergo treatment, 6) Recovered humans can become susceptible again, 7) All humans and vectors born are considered susceptible, 8) Infected vectors cannot be cured, 9) Human and vector deaths are natural, not due to disease, 10) the environment is implicitly reflected. Thus, the above assumptions can be visualized with a compartment diagram of the spread of Leptospirosis disease as in figure 1.

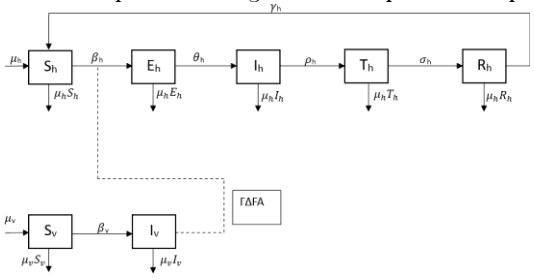

Figure 1. Compartmental Diagram of SEITR – SI Model.

2.2 Differential Equation System

From the image above, the dynamics of the model are expressed in the following differential equation system:

$$\frac{dS_h}{dt} = \mu_h N_h - \mu_h S_h - \beta_h I_v S_h + \gamma_h R_h, \quad (1)$$

$$\frac{dE_h}{dt} = \beta_h I_v S_h - \mu_h E_h - \theta_h E_h, \quad (2)$$

$$\frac{dI_h}{dt} = \theta_h E_h - \mu_h I_h - \rho_h I_h, \quad (3)$$
$$\frac{dT_h}{dt} = \rho_h I_h - \mu_h T_h - \sigma_h T_h, \quad (4)$$
$$\frac{dR_h}{dt} = \sigma_h T_h - \mu_h R_h - \gamma_h R_h, \quad (5)$$
$$\frac{dS_v}{dt} = \mu_v N_v - \mu_v S_v - \beta_v I_v S_v, \quad (6)$$
$$\frac{dI_v}{dt} = \beta_v I_v S_v - \mu_v I_v, \quad (7)$$

All model parameters are assumed to be positive for $t > 0$, with nonnegative initial conditions for all state variables. Parameter definitions and biological interpretations are summarized in Table 1.

Table 1. Parameter Description

Parameter	Description
μ_h	Natural birth and death rates of humans
N_h	Total human population
β_h	The rate of disease transmission from infected vectors to humans
θ_h	The rate at which humans move from exposure to infection
ρ_h	Rate of admission of infected humans to treatment
σ_h	Human recovery rate after treatment
γ_h	The rate at which people lose their immunity
μ_v	Natural birth and death rates vector
N_v	Total number of vector population
β_v	Rate of infection transmission in vectors

2.3 Equilibrium Point

The disease-free and endemic equilibrium point are determined analytically. Local stability of the disease-free equilibrium is analyzed using the Jacobian matrix and the basic reproduction number R_0. Due to high order of the characteristic equation at the endemic equilibrium, the Routh – Hurwitz criterion is employed to determine local asymptotic stability without explicitly computing all eigen values.

2.4 Basic Reproduction Number R_0

Basic reproduction number R_0 defined as the average number of new individuals infected by one infected individual in a fully susceptible population. Mark R_0 acts as a threshold parameter in epidemiological models. If $R_0 < 1$, then the disease will become extinct, whereas if $R_0 > 1$, the disease has the potential to become endemic.

2.5 Jacobian Matrix & Linearization

To analyze the local stability of equilibrium points, the system is linearized by calculating the Jacobian matrix. Let $X = (S_h, E_h, I_h, T_h, R_h, S_v, I_v)^T$. The Jacobian matrix $J(X)$ is defined as $J_{ij} = \partial f_i / \partial x_j$, where f_i denotes the right-hand side of system (1)–(7). Denote the Jacobian matrix of the system, where f_i represents the right-hand side of the differential equation and x_j denotes the state variables. The Jacobian matrix is evaluated at disease-free and endemic equilibrium points.

2.6 Stability Analysis

The local stability of equilibrium points is determined using eigenvalue analysis. For endemic equilibria, the Routh–Hurwitz criterion is used to assess the sign of the real part of the eigenvalues without explicitly calculating them.

2.7 Numerical Simulation

Numerical simulations are conducted to illustrate the analytical stability results rather than to provide empirical predictions. Constant values of β_h are used to represent different average hydroclimatic transmission intensities. The system is solved numerically using the ODEINT method in Python for both $R_0 < 1$ and $R_0 > 1$ scenarios to observe convergence toward disease-free and endemic equilibria. Although real environmental time-series data are not incorporated, such data may be used in future studies for model calibration and location-specific risk assessment.

3. RESULT AND DISCUSSION

3.1. Equilibrium Point

To determine the equilibrium point as a solution of the mathematical model expressed in a system of nonlinear ordinary differential equations, each derivative is equated to zero [26], [27]. Thus, the equilibrium points of the system are obtained, namely the disease-free equilibrium point (DFE) and the endemic equilibrium point (EE) which satisfy,

$$\frac{dS_h}{dt} = \frac{dE_h}{dt} = \frac{dI_h}{dt} = \frac{dT_h}{dt} = \frac{dR_h}{dt} = \frac{dS_v}{dt} = \frac{dI_v}{dt} = 0$$

By substituting the condition of no infected individuals, namely $E_h = I_h = T_h = R_h = I_v = 0$, the disease-free equilibrium point (DFE) is obtained as follows:

$$E^0 = (N_h, 0,0,0,0, N_v, 0)$$

Furthermore, if there is a condition of infected individuals, the endemic equilibrium point is obtained which is stated as follows:

$$E^* = (S_h{}^*, E_h{}^*, I_h{}^*, T_h{}^*, R_h{}^*, S_v{}^*, I_v{}^*),$$
$$\text{With}: S_h{}^* > 0, E_h{}^* > 0, I_h{}^* > 0, T_h{}^* > 0, R_h{}^* > 0, S_v{}^* > 0, I_v{}^* > 0.$$

Where (EE) includes:

$$S_v{}^* = \frac{\mu_v}{\beta_v};\ I_v{}^* = N_v - \frac{\mu_v}{\beta_v};\ S_h{}^* = \frac{\mu_h N_h + \gamma_h R_h}{\mu_h + \beta_h\left(N_h - \frac{\mu_v}{\beta_v}\right)};\ E_h{}^* = \frac{\beta_h\left(\frac{\mu_h N_h + \gamma_h R_h}{\mu_h + \beta_h\left(N_h - \frac{\mu_v}{\beta_v}\right)}\right)\left(N_v - \frac{\mu_v}{\beta_v}\right)}{\mu_h + \theta_h};$$

$$I_h{}^* = \frac{\theta_h \beta_h\left(\frac{\mu_h N_h + \gamma_h R_h}{\mu_h + \beta_h\left(N_h - \frac{\mu_v}{\beta_v}\right)}\right)\left(N_v - \frac{\mu_v}{\beta_v}\right)}{(\mu_h + \theta_h)(\mu_h + \rho_h)};\ T_h{}^* = \frac{\rho_h \theta_h \beta_h\left(\frac{\mu_h N_h + \gamma_h R_h}{\mu_h + \beta_h\left(N_h - \frac{\mu_v}{\beta_v}\right)}\right)\left(N_v - \frac{\mu_v}{\beta_v}\right)}{(\mu_h + \theta_h)(\mu_h + \rho_h)(\mu_h + \sigma_h)};\ R_h{}^* = \frac{\sigma_h \rho_h \theta_h \beta_h\left(N_v - \frac{\mu_v}{\beta_v}\right)}{(\mu_h + \theta_h)(\mu_h + \rho_h)(\mu_h + \sigma_h)\left[\mu_h + \beta_h\left(N_v - \frac{\mu_v}{\beta_v}\right)\right]}.$$

Since the characteristic polynomial of the endemic equilibrium is of degree four and algebraically intractable, the Routh–Hurwitz criterion is employed to assess local asymptotic stability [28]. Based on the calculation, with the condition $a_0 > 0, a_1 > 0, a_2 > 0, a_3 > 0, a_4 > 0$, also $b_1 > 0$ and $c_1 > 0$ that all roots of the polynomial have negative real parts and the endemic equilibrium point is locally asymptotically stable. This analysis will be further explored through numerical simulations which will be discussed next.

3.2. Basic Reproduction Number R_0

The basic reproduction number is determined using the Next Generation Matrix (NGM) by selecting subpopulations that spread the disease, namely E_h, I_h and I_v. From the system of ordinary differential equations, the Jacobian matrix is obtained, namely:

$$J(E_h, I_h, I_v) = \begin{bmatrix} -(\mu_h + \theta_h) & 0 & \beta_h N_h \\ \theta_h & -(\mu_h + \rho_h) & 0 \\ 0 & 0 & \beta_v N_v - \mu_v \end{bmatrix}$$

Then $J(E_h, I_h, I_v)$ it is stated $F - V$ that, where F is the transmission matrix or the matrix with the rate of new infections generated by infected individuals, while V is a matrix that shows the death rate or transition between infectious subpopulations.

$$F - V = \begin{bmatrix} 0 & 0 & \beta_h N_h \\ 0 & 0 & 0 \\ 0 & 0 & \beta_v N_v \end{bmatrix} - \begin{bmatrix} \mu_h + \theta_h & 0 & 0 \\ -\theta_h & \mu_h + \rho_h & 0 \\ 0 & 0 & \mu_v \end{bmatrix}$$

The inverse of matrix V is obtained as,

$$V^{-1} = \begin{bmatrix} \frac{1}{\mu_h + \theta_h} & 0 & 0 \\ \frac{\theta_h}{(\mu_h + \theta_h)(\mu_h + \rho_h)} & \frac{1}{\mu_h + \rho_h} & 0 \\ 0 & 0 & \frac{1}{\mu_v} \end{bmatrix}$$

The basic reproduction number is defined as the maximum eigenvalue of FV^{-1}, then evaluated at E^0. So, the value of the basic reproduction number R_0 is

$$R_0 = \frac{\beta_v N_v}{\mu_v}.$$

The basic reproduction number in this model is dominated by infection dynamics in the vector population, as vectors act as the primary source of infection and do not recover. Therefore, the vector subsystem contributes the most to the R_0 value. This result arises from the assumption that transmission occurs only from vectors to humans, while human-to-human and human-to-vector transmissions are neglected. Consequently, the basic reproduction number is governed solely by the infection dynamics of the vector population.

3.3. Local Stability of Disease-Free & Endemic Equilibria

A disease-free equilibrium point is declared locally stable if all eigenvalues of the Jacobian matrix have negative real values, indicating that the system will naturally maintain a disease-free state even if there is a disturbance at its critical point. These eigenvalues are obtained by constructing the Jacobian matrix based on the partial derivatives of equations (1) - (7) at the disease-free equilibrium point.

$$E^0 = (N_h, 0,0,0,0, N_v, 0)$$

The Jacobian matrix is obtained as follows.

$$J(E_0) = \begin{bmatrix} -\mu_h & 0 & 0 & 0 & \gamma_h & 0 & -\beta_h N_h \\ 0 & -\mu_h-\theta_h & 0 & 0 & 0 & 0 & \beta_h N_h \\ 0 & \theta_h & -\mu_h-\rho_h & 0 & 0 & 0 & 0 \\ 0 & 0 & \rho_h - \mu_h & -\sigma_h & 0 & 0 & 0 \\ 0 & 0 & 0 & \sigma_h & -\mu_h - \gamma_h & 0 & 0 \\ 0 & 0 & 0 & 0 & 0 & -\mu_v & -\beta_v N_v \\ 0 & 0 & 0 & 0 & 0 & 0 & \beta_v N_v - \mu_v \end{bmatrix}$$

So, the eigenvalue of the Jacobian matrix is obtained as:

$$\lambda_1 = -\mu_h - \gamma_h,\ \lambda_2 = -\mu_v, \lambda_3 = \beta_v N_v - \mu_v,\ \lambda_4 = -\sigma_h, \lambda_5 = -\mu_h - \rho_h,$$
$$\lambda_6 = -\mu_h - \theta_h,\ \lambda_7 = -\mu_h.$$

For the disease-free equilibrium point to be stable, all eigenvalues must be negative. This condition is met if,

$$\lambda_3 = \beta_v N_v - \mu_v < 0,$$

Which is equivalent to,

$$\frac{\beta_v N_v}{\mu_v} < 1.$$

Thus, all eigenvalues of the Jacobian matrix at the disease-free equilibrium point are negative. Therefore, the disease-free equilibrium point in the leptospirosis distribution model is asymptotically stable.
However, if

$$\frac{\beta_v N_v}{\mu_v} > 1.$$

Then point DFE becomes unstable and point EE becomes stable. Thus, based on the Routh–Hurwitz criterion, all roots of the polynomial have negative real parts, so the endemic equilibrium point is asymptotically stable. Numerical simulations are then used to verify the analysis results.

3.4. Numerical Simulation

Numerical simulations are conducted to illustrate the theoretical stability properties of the proposed model rather than to simulate explicit time-varying hydroclimatic processes. Although β_h conceptually represents hydroclimatic variability, it is treated as a constant parameter in this autonomous framework. Therefore, variations in hydroclimatic effects are reflected through changes in the magnitude of β_h, rather than through explicit time-dependent or data-driven $\beta_h(t)$.

The parameters used in the numerical simulations were obtained from several literature sources [18], [24], [29], [30] and used to illustrate the theoretical behavior of the model. The parameter values used for the disease-free equilibrium (DFE) point are presented in table 2.

Table 2. Values for DFE

Parameter	Mark	Reference	Dimensions
μ_h	0.02	[29]	/day
N_h	100	[18]	/day
β_h	0.5	[29]	/day
θ_h	0.2	[29]	/day
ρ_h	0.1	[30]	/day
σ_h	0.1	[30]	/day
γ_h	0.05	[30]	/day
μ_v	1.2	[24]	/day
N_v	100	[18]	/day
β_v	0.001	[30]	/day

Numerical simulations were performed based on the parameter values listed in Table 2. As the initial conditions $S_h(0) = 50, E_h(0) = 15, I_h(0) = 15, T_h(0) = 10, R_h(0) = 10, S_v(0) = 60, I_v(0) = 40$. The system of nonlinear ordinary differential equations was solved numerically by the odeint method in Python. The results of the numerical simulations are presented in graphical form to illustrate the dynamic behavior of each compartment over time.

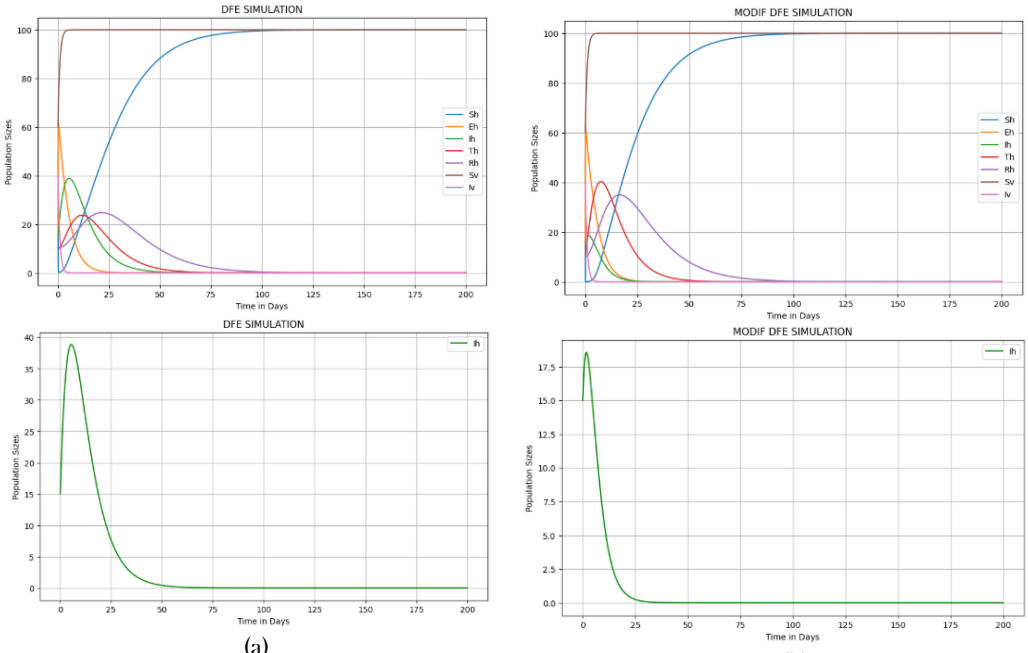

(a) (b)

Figure 2. Numerical simulation of the SEITR–SI model under conditions $R_0 < 1$.
Panel (a) shows the time evolution of all human and vector compartments.
Panel (b) illustrates the corresponding dynamics under modified hydroclimatic transmission intensity.

A numerical disease-free stability analysis is obtained by using the parameters in Table 2, based on the eigenvalues of the Jacobian matrix, namely:

$$\lambda_1 = -0.07,\ \lambda_2 = -1.2,\ \lambda_3 = -1.1,\ \lambda_4 = -0.1, \lambda_5 = -0.12,\ \lambda_6 = -0.22,\ \lambda_7 = -0.02.$$

Since all the eigenvalues obtained are negative, the disease-free equilibrium point is asymptotically stable. Furthermore, the basic reproduction number is obtained as follows, $R_0 = 0.083$.

Based on Figure 2(a), the dynamics of each subpopulation are observed over a 200-day period. The susceptible human subpopulation (S_h) and the susceptible vector subpopulation (S_v) increased significantly. In contrast, the exposed human subpopulation (E_h), the infected human subpopulation, (I_h), the treated human subpopulation (T_h), the recovered human subpopulation (R_h), and the infected vector subpopulation (I_v) showed a significant decline and moved towards zero over time.

Based on Figure 2(b), if the value of (ρ_h), is modified to 0.5 and the value of (β_h) modified to 2.5, then causes an increase in the (T_h), part slightly then towards zero over time while (E_h), (I_h), and (R_h) experiences a faster decrease than in Figure 2a towards zero over time.

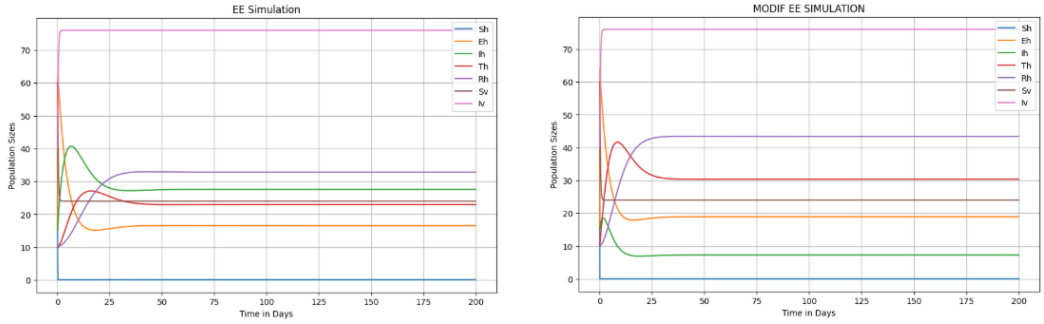

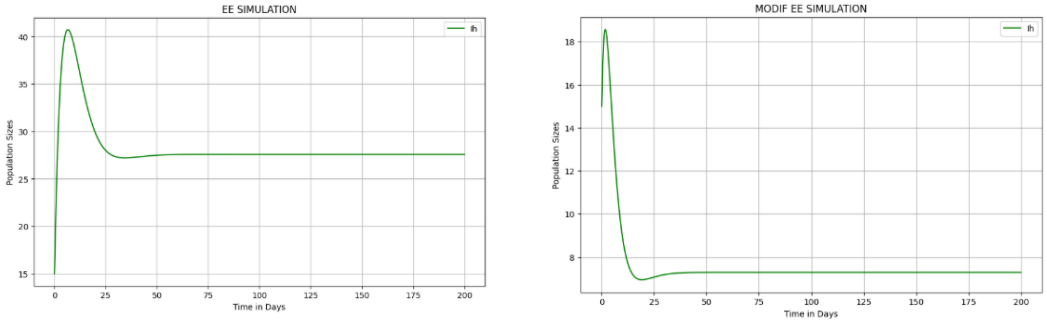

(a) (b)

Figure 3. Numerical simulation of the SEITR–SI model under conditions $R_0 > 1$.
Panel (a) illustrates the temporal dynamics of all model compartments,
Panel (b) depicts the system behavior under higher hydroclimatic transmission intensity.

The parameters in Table 2 were used, modifications were made to the vector transmission rate of $\beta_v = 0.05$ and based on the calculation results using the Routh–Hurwitz criteria, it was obtained that the endemic equilibrium point is asymptotically stable with a basic reproduction number value of $R_0 = 4.167$.

At the endemic equilibrium point, the Jacobian matrix exhibits a block structure, allowing three eigenvalues to be obtained directly. The remaining four eigenvalues are associated with a reduced subsystem that leads to a fourth-degree characteristic polynomial of the form $\lambda^4 + a_3\lambda^3 + a_2\lambda^2 + a_1\lambda + a_0 = 0$. Due to the algebraic complexity of this polynomial, explicit analytical expressions for its roots are not derived. Therefore, the local stability of the endemic equilibrium point is examined using the Routh–Hurwitz criterion.

$$a_2 = \left(\left(N_v - \frac{\mu_v}{\beta_v}\right)(\beta_h)\right)(\gamma_h + 3\mu_h + \rho_h + \sigma_h + \theta_h) + ((\gamma_h)(3\mu_h + \rho_h + \sigma_h + \theta_h)) + \big((3\mu_h)(2\mu_h + 3\rho_h + 3\sigma_h + 3\theta_h)\big) + \big((\rho_h)(\sigma_h + \theta_h)\big) + \sigma_h\theta_h\,, \quad (8)$$

$$a_1 = \left(\left(\left(N_v - \frac{\mu_v}{\beta_v}\right)(\beta_h)(\gamma_h)\right)(2\mu_h + 3\rho_h + 3\sigma_h + 3\theta_h)\right) + \left(\left(\left(N_v - \frac{\mu_v}{\beta_v}\right)(\beta_h)(\rho_h)\right)(2\sigma_h + 2\theta_h)\right) + \left(\left(N_v - \frac{\mu_v}{\beta_v}\right)(\beta_h)(\sigma_h)(\theta_h)\right) + \big((2\gamma_h\mu_h)(\rho_h + \sigma_h + \theta_h)\big) + \Big(\big((\gamma_h\rho_h)(\sigma_h + \theta_h)\big) + \gamma_h^2\theta_h + \big((\rho_h\theta_h)(2\mu_h + \sigma_h)\big)\Big), \quad (9)$$

$$a_0 = \left(\left(\left(N_v - \frac{\mu_v}{\beta_v}\right)(\beta_h)(\gamma_h)\right)(\mu_h^2 + \mu_h\rho_h + \mu_h\sigma_h + \mu_h\theta_h)\right) + \left(\left(\left(N_v - \frac{\mu_v}{\beta_v}\right)(\beta_h)(\gamma_h)\right)(\rho_h\sigma_h + \rho_h\theta_h + \sigma_h\theta_h)\right) + \left(\left(\left(N_v - \frac{\mu_v}{\beta_v}\right)(\beta_h)(\mu_h)\right)(\mu_h^2 + \mu_h\rho_h + \mu_h\sigma_h + \mu_h\theta_h + \rho_h\sigma_h + \rho_h\theta_h + \sigma_h\theta_h)\right) + \left(\left(N_v - \frac{\mu_v}{\beta_v}\right)(\beta_h)(\rho_h)(\sigma_h)(\theta_h)\right) + ((\gamma_h\mu_h)(\mu_h^2 + \mu_h\rho_h + \mu_h\sigma_h + \mu_h\theta_h + \rho_h\sigma_h + \rho_h\theta_h + \sigma_h\theta_h)) + (\gamma_h\rho_h\sigma_h\theta_h) + \mu_h^4 + \Big((\mu_h^3)(\rho_h + \sigma_h + \theta_h)\Big) + \Big((\mu_h^2)(\rho_h\sigma_h + \rho_h\theta_h + \sigma_h\theta_h)\Big) + (\mu_h\rho_h\sigma_h\theta_h), \quad (10)$$

Table 3. Values for Routh – Hurwitz.

Quantity	Expression	Numerical value	Sign
a_4	1	1	> 0
a_3	$4\mu_h + \sigma_h + \theta_h + \left(N_v - \frac{\mu_v}{\beta_v}\right)\beta_h + \gamma_h$	38.43	> 0
a_2	See Eq (8)	19.53	> 0
a_1	See Eq (9)	5.4	> 0
a_0	See Eq (10)	0.23	> 0
b_1	$\frac{a_3a_2 - a_4a_1}{a_3}$	19.39	> 0
b_2	See Eq (10)	0.23	> 0
c_1	$\frac{b_1a_1 - a_3a_0}{b_1}$	4.94	> 0

Since all coefficients and leading principal minors in the Routh–Hurwitz table are positive, the endemic equilibrium point is locally asymptotically stable.

Based on Figure 3(a), when $R_0 > 1$ within a 200-day period, it was observed that human subpopulations were susceptible (S_h) and susceptible rat subpopulations (S_v) experienced a decline towards a point of stability. In addition, subpopulations of exposed humans (E_h), infected humans (I_h), treated humans (T_h), recovered humans (R_h), and subpopulations of infected vector (I_v) also indicate convergence towards a stable endemic equilibrium.

Then in Figure 3(b), by modifying the rate of disease transmission from infected vectors to humans by $\beta_h = 2.5$ and the rate of human treatment by $\rho_h = 0.5$, it is shown that the hydroclimatic rate and the treatment rate significantly increases the treated population (T_h), while the exposed, infected, and recovered human populations increase but converge to lower endemic equilibrium levels compared to Figure 3(a).

This study is primarily theoretical in nature and focuses on analytical stability properties of the proposed autonomous system rather than empirical calibration. The exclusion of time-series hydroclimatic data is intentional, as incorporating explicit environmental forcing would transform the model into a non-autonomous system and significantly alter the stability framework. Therefore, the numerical simulations are designed to support qualitative theoretical insights rather than location-specific quantitative prediction.

3.5. Discussion

The proposed SEITR–SI model confirms the threshold behavior governed by the basic reproduction number R_0, determining the local stability of the disease-free and endemic equilibria. Similar threshold dynamics have been reported in SEIR–SI and SIR–SI models such as [24] and [25]. However, unlike [24], which excludes treatment dynamics, and [25], which incorporates hydroclimatic effects explicitly in rodent infection rates, the present model integrates treatment and hydroclimatic transmission intensity within a unified and analytically tractable framework.

Although R_0 is primarily determined by vector transmission parameters, numerical simulations indicate that the hydroclimatic transmission parameter β_h substantially increases the endemic equilibrium level of infected humans. Thus, hydroclimatic intensity may not directly modify the epidemic threshold but significantly amplifies disease persistence once $R_0 > 1$. These findings suggest that treatment alone may not be sufficient to eliminate leptospirosis in hydroclimate-sensitive environments.

From a public health perspective, the results highlight the necessity of integrated control strategies. In addition to treatment, effective leptospirosis prevention should include environmental sanitation, rodent population control, improved drainage systems, and early warning measures during periods of heavy rainfall or flooding. Such integrated approaches are particularly important in regions where hydroclimatic conditions intensify environmental transmission pathways.

This study is limited to local stability analysis and does not incorporate empirical hydroclimatic time-series data. Therefore, the results provide qualitative theoretical insights rather than quantitative predictive estimates. Future work may extend the present framework by integrating rainfall or flood occurrence data to evaluate how temporal variability in hydroclimatic conditions influences threshold behavior and long-term disease dynamics.

4. CONCLUSION

This study provides qualitative insights into leptospirosis dynamics through a SEITR–SI model incorporating hydroclimate-dependent transmission and treatment. The analysis shows that the disease-free equilibrium is locally asymptotically stable when $R_0 < 1$, while a stable endemic equilibrium exists when $R_0 > 1$.

Numerical simulations indicate that increasing the hydroclimatic transmission parameter β_h raises endemic infection levels, even under higher treatment rates, suggesting that environmentally driven transmission can sustain persistence despite medical intervention.

These results imply that effective control in hydroclimate-sensitive regions should combine treatment with environmental risk reduction. Practical strategies include improved drainage in flood-prone areas, seasonal rodent control during high-rainfall periods, strengthened sanitation to reduce contaminated water exposure, and integration of epidemiological surveillance with rainfall and flood monitoring systems to anticipate elevated transmission risk. Enhancing early diagnosis and rapid treatment during such periods may further reduce endemic persistence.

Although this study focuses on local stability analysis without empirical hydroclimatic data, the framework provides a theoretical foundation for integrated medical and environmental control strategies in climate-sensitive settings.

5. REFERENCES

[1] J. E. Hagan et al., "Spatiotemporal Determinants of Urban Leptospirosis Transmission: Four-Year Prospective Cohort Study of Slum Residents in Brazil," PLoS Negl. Trop. Dis., vol. 10, no. 1, Jan. 2016, doi: 10.1371/journal.pntd.0004275.

[2] Antima and S. Banerjee, "Modeling the dynamics of leptospirosis in India," Sci. Rep., vol. 13, no. 1, Dec. 2023, doi: 10.1038/s41598-023-46326-2.

[3] H. Qu, S. Saifullah, J. Khan, A. Khan, M. Ur Rahman, and G. Zheng, "DYNAMICS OF LEPTOSPIROSIS DISEASE IN CONTEXT OF PIECEWISE CLASSICAL-GLOBAL AND CLASSICAL-FRACTIONAL OPERATORS," Fractals, vol. 30, no. 8, Dec. 2022, doi: 10.1142/S0218348X22402162.

[4] A. G. Regassa and L. L. Obsu, "The role of asymptomatic cattle for leptospirosis dynamics in a herd with imperfect vaccination," Sci. Rep., vol. 14, no. 1, Dec. 2024, doi: 10.1038/s41598-024-72613-7.

[5] B. A. Miotto et al., "Prospective study of canine leptospirosis in shelter and stray dog populations: Identification of chronic carriers and different Leptospira species infecting dogs," PLoS One, vol. 13, no. 7, Jul. 2018, doi: 10.1371/journal.pone.0200384.

[6] M. Said, Y. Roh, and I. H. Jung, "Mathematical modeling and analysis of leptospirosis–COVID-19 co-infection with real data," Eur. Phys. J. Plus, vol. 139, no. 11, Nov. 2024, doi: 10.1140/epjp/s13360-024-05846-0.

[7] D. Sutiningsih et al., "Geospatial Analysis of Abiotic and Biotic Conditions Associated with Leptospirosis in the Klaten Regency, Central Java, Indonesia," Trop. Med. Infect. Dis., vol. 9, no. 10, Oct. 2024, doi: 10.3390/tropicalmed9100225.

[8] I. Ridha, R. #1, and M. Subhan, "Pemodelan Matematika Penyebaran Penyakit Leptospirosis dengan Pengaruh Treatment."

[9] D. Benacer et al., "Determination of Leptospira borgpetersenii serovar Javanica and Leptospira interrogans serovar Bataviae as the persistent Leptospira serovars circulating in the urban rat populations in Peninsular Malaysia," Parasit. Vectors, vol. 9, no. 1, Mar. 2016, doi: 10.1186/s13071-016-1400-1.

[10] S. Chadsuthi, K. Chalvet-Monfray, A. Wiratsudakul, and C. Modchang, "The effects of flooding and weather conditions on leptospirosis transmission in Thailand," Sci. Rep., vol. 11, no. 1, Dec. 2021, doi: 10.1038/s41598-020-79546-x.

[11] S. Sánchez-Montes, D. V. Espinosa-Martínez, C. A. Ríos-Muñoz, M. Berzunza-Cruz, and I. Becker, "Leptospirosis in Mexico: Epidemiology and potential distribution of human cases," PLoS One, vol. 10, no. 7, Jul. 2015, doi: 10.1371/journal.pone.0133720.

[12] M. Garcia-Lopez et al., "Prevalence, genetic diversity and ecoepidemiology of pathogenic Leptospira species in small mammal communities in urban parks Lyon city, France," PLoS One, vol. 19, no. 4 April, Apr. 2024, doi: 10.1371/journal.pone.0300523.

[13] M. Farman, S. Jamil, K. S. Nisar, and A. Akgul, "Mathematical study of fractal-fractional leptospirosis disease in human and rodent populations dynamical transmission," Ain Shams Engineering Journal, vol. 15, no. 3, Mar. 2024, doi: 10.1016/j.asej.2023.102452.

[14] V. Saravanan, R. Chinnathambi, and F. A. Rihan, "Modeling and controlling Leptospirosis transmission in humans and rodents," Journal of Mathematics and Computer Science, vol. 39, no. 1, pp. 30–49, 2025, doi: 10.22436/jmcs.039.01.03.

[15] P. Rohani, C. J. Green, N. B. Mantilla-Beniers, and B. T. Grenfell, "Ecological interference between fatal diseases," Nature, vol. 422, no. 6934, pp. 885–888, Apr. 2003, doi: 10.1038/nature01542.

[16] M. Sooryadas, A. L. Haseena, S. Selsha, and K. Balachandran, "Stability analysis of leptospirosis compartmental model with impact of contaminated environment," Nonlinear Analysis: Modelling and Control, vol. 30, no. 5, pp. 957–981, 2025, doi: 10.15388/NAMC.2025.30.42973.

[17] A. Khan, A. Raouf, R. Zarin, A. Yusuf, and U. W. Humphries, "Existence theory and numerical solution of leptospirosis disease model via exponential decay law," AIMS Mathematics, vol. 7, no. 5, pp. 8822–8846, 2022, doi: 10.3934/math.2022492.

[18] Ministry of Health of the Republic of Indonesia, Leptospirosis Situation in Indonesia 2024, Jakarta Ministry of Health, 2024.

[19] S. J. Jahja and C. Drew, "Peningkatan Pengetahuan dalam Upaya Pencegahan Kasus Baru Leptospirosis di Wilayah Kerja Puskesmas Kresek," Malahayati Nursing Journal, vol. 6, no. 2, pp. 725–735, Feb. 2024, doi: 10.33024/mnj.v6i2.12875.

[20] S. H. Ideris, N. Shaadan, S. N. Shair, and N. A. Samat, "Leptospirosis Relative Risk Estimates based on Continuous-Time, Discrete-Space Stochastic SIR-L-SI Transmission Model," Malaysian Journal of Fundamental and Applied Sciences, vol. 20, no. 1, pp. 223–246, Jan. 2024, doi: 10.11113/mjfas.v20n1.3182.

[21] S. Khan, Z. A. Khan, H. Alrabaiah, and S. Zeb, "On Using Piecewise Fractional Differential Operator to Study a Dynamical System," Axioms, vol. 12, no. 3, Mar. 2023, doi: 10.3390/axioms12030292.

[22] B. S. T. Alkahtani and S. S. Alzaid, "Studying the Dynamics of the Rumor Spread Model with Fractional Piecewise Derivative," Symmetry (Basel)., vol. 15, no. 8, Aug. 2023, doi: 10.3390/sym15081537.
[23] F. K. Alalhareth, U. Atta, A. H. Ali, A. Ahmad, and M. H. Alharbi, "Analysis of Leptospirosis transmission dynamics with environmental effects and bifurcation using fractional-order derivative," Alexandria Engineering Journal, vol. 80, pp. 372–382, Oct. 2023, doi: 10.1016/j.aej.2023.08.063.
[24] A. Ahmad, U. Atta, A. Akgül, S. Sattar, and M. O. Ahmad, "A study on mathematical modeling and control of leptospirosis transmission dynamics during a hurricane with asymptomatic measures," Model. Earth Syst. Environ., vol. 11, no. 5, Oct. 2025, doi: 10.1007/s40808-025-02508-7.
[25] A. A. Gómez, M. S. López, G. V. Müller, L. R. López, W. Sione, and L. Giovanini, "Modeling of leptospirosis outbreaks in relation to hydroclimatic variables in the northeast of Argentina," Heliyon, vol. 8, no. 6, Jun. 2022, doi: 10.1016/j.heliyon.2022.e09758.
[26] N. K. Tokarevich and O. V Blinova, "Обзоры Reviews LEPTOSPIROSIS IN VIETNAM," Russian Journal of Infection and Immunity = Infektsiya i immunitet 2022, vol. 12, no. 6, pp. 1019–1028, doi: 10.15789/2220-7619.
[27] Amanda, "Zero : Jurnal Sains, Matematika, dan Terapan IMPLEMENTATION OF SIR MODEL IN THE SPREAD OF TB INFECTIOUS DISEASES IN PEMATANGSIANTAR CITY," vol. 5, no. 1, pp. 14–21, 2021.
[28] N. Fiska, M. Ikhwan, N. Nurmaulidar, and O. Askal, "Routh-Hurwitz Stability Analysis of the Predator-Prey Model with Prey Population Harvesting in Polluted Aquatic Ecosystems," ZERO: Jurnal Sains, Matematika dan Terapan, vol. 9, no. 2, p. 575, Oct. 2025, doi: 10.30829/zero.v9i2.26061.
[29] H. A. Engida, D. M. Theuri, D. Gathungu, J. Gachohi, and H. T. Alemneh, "A Mathematical Model Analysis for the Transmission Dynamics of Leptospirosis Disease in Human and Rodent Populations," Comput. Math. Methods Med., vol. 2022, 2022, doi: 10.1155/2022/1806585.
[30] R. Artiono et al., "Mathematical Analysis and Numerical Simulation on Free-Living Leptospira: A Mathematical Modeling Perspective," European Journal of Pure and Applied Mathematics, vol. 17, no. 3, pp. 1637–1658, Jul. 2024, doi: 10.29020/nybg.ejpam.v17i3.5178.